International Journal of
INTELLIGENT SYSTEMS AND APPLICATIONS IN ENGINEERING
ISSN:2147-6799 www.ijisae.org Original Research Paper

Static Weather Image Classification Based on Fog Aware Statistical Features Using XGBoost Classifier

Padmini T. N*[1], Shankar T[2]

Submitted: 22/**0**7/**2022** **Accepted:** 25/**0**9/**2022**

Abstract: The outdoor functions carried out by the autonomous navigation systems fail in extreme weather conditions. To tide over such issues, many researchers have implemented an algorithm to get rid of the fog, rain and snow from images. Most of the dehazing algorithms are implemented by researchers considering the input image as a hazy image. But in the real-time scenario, the image captured by the camera can be any image with or without degradation due to the influence of the weather. This research is a proposal to classify static weather images like haze and fog along with sunny images using a supervised classifier. It can be stated that this is a pioneering opportunity to analyze fog and haze as two separate classes. Other researchers have hitherto treated them as just one class. The proposed method was implemented by collecting images from existing databases and forming a new database by relabeling the images as haze and fog based on psycho-visual analysis. The classification model was trained and tested on static weather images using a supervised classifier. It was inferred that the XGBoost classifier has a definite edge over such other classifiers in existence.

Keywords: *Dehazing, Feature extraction, Machine learning, supervised classifier, XGBoost classifier*

1. Introduction

Weather conditions can be classified into two namely static and dynamic types. Haze, fog and sunny images can be categorized under static, while rain and snow are categorized under dynamic [1]. Haze and fog differ based on their densities. Haze is mild whereas fog is dense. Fig.1 shows sample images differentiating sunny, hazy, and foggy. The contrast and color are degraded in the foggy image when compared with the hazy and sunny images.

In the dehazing algorithm [2] or deraining algorithm [3], the input is assumed to be a hazy or a rainy image. In the real-time scenario, these algorithms are difficult to implement because the input can be any image, with or without degradation, due to the weather conditions. Very few researchers have worked in this area of classifying different weather degraded images due to the lack of availability of datasets. Some researchers have used synthetic images for classifying and some of them have used scene-specific images like road images focusing on intelligent transport systems. The challenge in this field of classification is to discriminate the weather images by extracting appropriate features. Recently a few researchers have started to work in this field by classifying the weather images.

Most of the dehazing algorithms remove only haze but not fog from the images. To feed only hazy images to the dehazing algorithm, haze and foggy images should be discriminated. As an initiative, this research work proposes a multi-class classification technique to categorize static weather images like haze, fog and sunny images using colour images of natural outdoor scenes.

[1] *Department of Embedded Technology, Vellore Institute of Technology, Vellore, India*
ORCID ID : 0000-0001-7642-2283
[2] *Department of Communication Engineering, Vellore Institute of Technology, Vellore, India*
ORCID ID : 0000-0003-3532-2782
** Corresponding Author Email: tnpadmini@vit.ac.in*

2. Related Work

A few researchers have worked in this area of classification of weather images which is reviewed in this section. Hautiere et al. [4] have proposed a method to detect fog and estimate the visibility distance from the images depicting a road scene with the sky, using an on-board camera. The approach is based on Koschmieder's mathematical model which can detect only daytime fog. Lagorio et al. [5] have proposed a method based on a mixture of Gaussian models to detect fog, snow, and heavy rain by identifying spatial and temporal frequency changes. The drawback of this method is that it requires information like camera optics and viewing distance. Negru and Nedevschi [6] have proposed a method to detect fog and estimated visibility distance to assist the drivers. This approach is based on an image processing technique using canny edge detection and then estimating the inflection point and horizon line to detect fog along with visibility distance. This model does not work for images with scenes depicting crowded roads. Shen and Tan [7] have proposed a simple method to detect sunny and cloudy weather conditions from the images based on global illumination. Cord and Aubert [8] have proposed a method

using an image processing technique, based on gradient variations, to detect raindrops from the windshield of vehicles using an on-board camera, based on photometric properties.

(a) (b) (c)

Fig. 1. Static weather images (a) Sunny (b) Hazy and (c) Foggy.

Roser and Moosmann [9] have proposed a method to classify sunny and rainy images using Support Vector Machine (SVM). Features like contrast, hue, brightness, sharpness, and saturation were extracted and classified based on Region of Interest (ROI). The limitation of this model is that it can detect only sunny and rainy images. Yan et al. [10] have proposed a method to classify weather images as sunny, cloudy, and rainy using a Histogram of gradient amplitude, as well as a Histogram of Hue Saturation Value (HSV) color space, and road information, to detect the features. After detecting the features, the images were classified using AdaBoost. This method is suitable for classifying images depicting only road scenes that are captured from on-board cameras in vehicles. Later, Elhoseiny et al. [11] used a Convolution Neural Network (CNN) to classify images, as sunny and cloudy. As larger data is required for better accuracy the size of the dataset was increased using data augmentation technique. Multi-kernel and dictionary learning techniques were suggested by Zheng Zhang et al. [12] to classify weather images as sunny, rainy, snowy, and hazy. They used features like the sky, shadow, rain streak, snow along with contrast and saturation to classify the weather images. Chu et al. [13] classified images using weather images through geotagging which includes information like weather type, temperature, and humidity. To summarize, the initial stage of this field of research concentrated on mathematical models using image processing techniques by detecting only fog which requires minimal data with user-defined settings that are less accurate. Later they moved to machine learning and deep learning techniques to classify weather images which are more accurate than the methods adopted earlier.

The challenge in classifying weather images is the lack of features discriminating the diverse weather conditions. Further, there have been no recent attempts in this research field due to the lack of availability of public datasets. The proposed method was implemented using machine learning techniques, by extracting features that could distinguish haze and fog, rather than using deep learning methods that require a large dataset.

3. Methodology

Supervised learning is generally used for image classification to train the model which maps from the independent input variable (X) to the dependent output variable (Y).There are two phases in supervised learning namely training phase and testing phase. In the training phase, the classification model is trained with a set of data known as training data. Once the model is trained it is tested using a test dataset. As shown in Fig. 2, the features were extracted from the training images and labelled. The model was trained with the help of features, so that it became a learned model. During the testing phase, the same features are extracted from the test image and fed to the learned model to predict and classify an image as sunny, hazy, or foggy accurately.

3.1. Weather image dataset

In the proposed method static weather images were initially collected. Since no public database differentiating haze and fog is available, the images were separated from the existing database to create a new database. Datasets were collected from the Wang et al. [14] database and Choi et al. [15] database which consisted of haze-free and hazy images. The database had both haze and fog images. Incidentally, most researchers use the terms haze and fog interchangeably.

The Wang et al. [14] dataset consisted of haze-free images with high-quality outdoor natural images which comprised of sunny, cloudy, and snowy images. All the haze-free images captured by the authors were of high contrast and free from haze or fog. The authors also collected hazy images from miscellaneous sources which included both haze and foggy images. Wang et al. [14] used subjective assessment obtained from 15 observers based on the perception and separated the hazy database into light, mild, and dense hazy images taking into consideration only the non-sky region. The images were classified by Wang et al. [14] based on maximum voting of an image obtained for a particular class by randomly displaying still images to the 15 observers. Based on their perception, the images were classified into light, mild and dense hazy images.

But the Wang et al. [14] classification did not account for the mild hazy images that lay in between light haze and dense haze resulting in redundant images. Thus, there were around 29 images in both light as well as mild haze. Similarly, 21 images were found in both mild as well as dense hazy images.

The database proposed by Choi et al. [15] is a small dataset that consists of fog-free and foggy images. Since the author has used the term foggy, here it is referred to as foggy images. But this database of foggy images consists of both haze and foggy images. Fog-free images are natural color images, mostly outdoor images which consist of sunny, cloudy and snowy which were obtained by the author from Sheikh et al. [16], Martin et al. [17], Callet et al. [18] and Larson et al. [19] databases. The size of the fog-free images

ranged from 480 x 320 to 770 x 512 pixels. The foggy images were taken from free web sources with fog density ranging from light to dense. Some images were obtained from Tan et al. [20], Fattal et al. [21], He et al. [22], Tarel et al.[23], Kratz et al. [24], Nishino et al. [25], Ancuti et al. [26] provided by the authors in their website. The image size of the foggy image ranged from 300 x 300 to 1128 x 752 pixels.

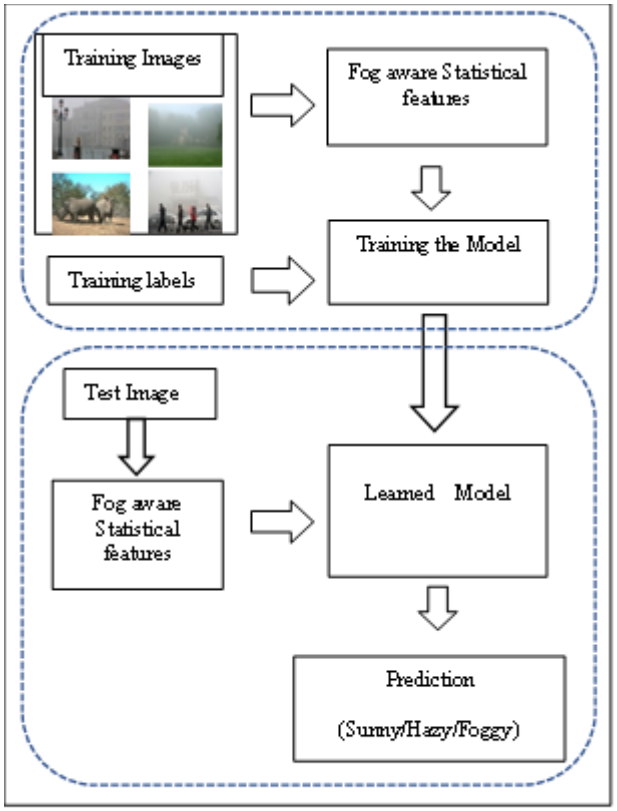

Fig. 2. Frame work of the proposed method depicting training and testing phase

A new database was formed from the existing database which included sunny, hazy and foggy images. Since Wang et al. [14] database had redundant images in the mild hazy image dataset which lay between light haze and dense haze, the redundant images were removed. The redundant images from the two databases were also removed as well as a few grayscale images. The images from Wang et al. [14] and Choi et al. [15] database were also separated into sunny, hazy, and foggy based on psycho-visual analysis with the help of 20 observers. Foggy images are denser than hazy where most of the background scenes in the images are invisible.

The images were differentiated based on depth, as the density of the fog or haze varies with depth. In some images the objects that are closer will be visible but distant ones will be invisible and are categorized as foggy images. But in the case of hazy images, both the nearby and distant objects will be visible but details are not clearly discernible. The new database consists of homogenous hazy and foggy images whereas, heterogeneous images are not considered. A sunny image dataset was formed from the existing haze-free

Fig. 3. Same background scene with different fog densities [15]

images excluding the cloudy and snowy images. The outdoor day-time color images with clear sky regions without clouds are considered as sunny images. Therefore, the images collected from the two databases were segregated into three classes based on color and contrast.

The sunny image is colorful with high contrast. But the color and contrast gradually deteriorated in the case of hazy and foggy images. A total of 2941 images were collected from the existing datasets and classified into three classes namely sunny, hazy, and foggy as shown in Table 1.

Table 1. Distribution Statistics of Weather Images

Label	Sunny	Hazy	Foggy	Total images
No of images	1510	589	842	2941

3.2. Feature Extraction from static weather images

Static weather images like hazy, foggy, and sunny images can be classified using machine learning algorithms in two steps. The first step is to extract the statistical features from the input static weather images followed by the second step which involves the classification techniques. Statistical features were extracted from the new dataset which had outdoor color images like sunny, hazy and foggy.

Choi et al. [15] introduced an evaluating tool known as Fog-Aware Density Evaluator (FADE) to evaluate the fog density in an image using the statistical features which was adopted by us. The features extracted from the images for the proposed method are as follows:

3.2.1. Mean Subtraction and Contrast Normalized (MSCN):

MSCN was obtained by subtracting the mean from the gray scale image intensity and dividing it by the standard deviation as specified by Choi et al. [15] in (1),

$$I(MSCN) = \frac{I(m,n) - \mu(m,n)}{\sigma(m,n)+1} \quad (1)$$

According to Choi et al. [15], MSCN was measured for images with the same background scene but with different fog densities ranging from dense fog to fog-free as shown in Fig. 3, and the histogram of the MSCN coefficient for Fig. 3 is depicted in Fig. 4.

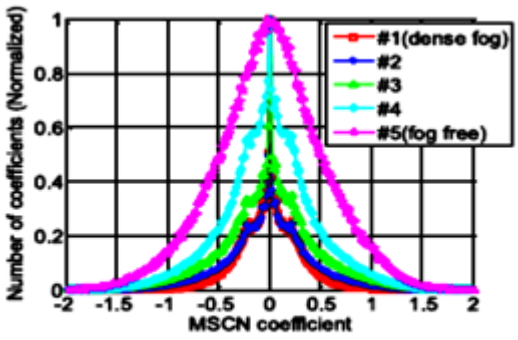

Fig. 4. Histogram of MSCN coefficients [15]

It was found that for a clear sunny image, the histogram plotted using MSCN coefficient was a normalized Gaussian curve and it was decorrelated whereas for a hazy or foggy image the shape of the curve was not perfect Gaussian and it was correlated as shown in Fig.4.

3.2.2. Sharpness:

The contrast of the sunny, hazy, foggy image was obtained by measuring the standard deviation.

3.2.3. Contrast Energy:

The local contrast of the image was computed as in (2) which is applied to grayscale, yellow-blue, and red-green planes separately [15]

$$CE(I) = \frac{\alpha.G(I)}{G(I)+\alpha.\beta} - \tau \quad (2)$$

where *G(I)* is the gradient magnitude obtained by convolving image with the second-order derivative of Gaussian function in horizontal and vertical directions, α is the maximum value of G(I), β is the contrast gain and τ is the noise threshold.

3.2.4. Entropy:

Entropy is used to predict the information present in an image and it was calculated as in (3) as specified by Choi et al., [15],

$$E = -\sum_x p(x)\log\left[p(x)\right] \quad (3)$$

where p(x) indicates the probability of the intensity of the pixel in an image.

3.2.5. Dark channel prior (DCP):

He et al. [22] introduced a novel concept known as dark channel prior, where the author found that the minimum pixel intensity obtained between the RGB channels of the color image was found predominantly dark for a clear image but for a hazy image it was not dark.

3.2.6. Saturation:

Air-light added with the reflected light from the scene in hazy or foggy images causes whiteness in the images which can be measured by converting the hazy or foggy image into Hue, Saturation and Value (HSV) plane and obtaining the measure from the saturation plane.

3.2.7. Colorfulness:

The deviation in color from gray, due to air-light can be calculated as specified by Choi et al. [15] as in (4) as follows

$$CF = \sqrt{\sigma^2_{(r-g)} + \sigma^2_{(y-b)}} + 0.3\sqrt{\mu^2_{(r-g)} + \mu^2_{(y-b)}} \quad (4)$$

where σ is standard deviation and μ is mean of red-green and yellow-blue plane respectively.

After extracting the statistical features from the new dataset the distribution of data between haze and fog was determined using a scatter plot.

Fig. 5 shows the scatter plot for different features with blue color dots indicating the features extracted from the foggy images and red color dots indicating the features extracted from the hazy images. From the scatter plot it was observed that except for the DCP all the features have a lower value for fog when compared with haze.

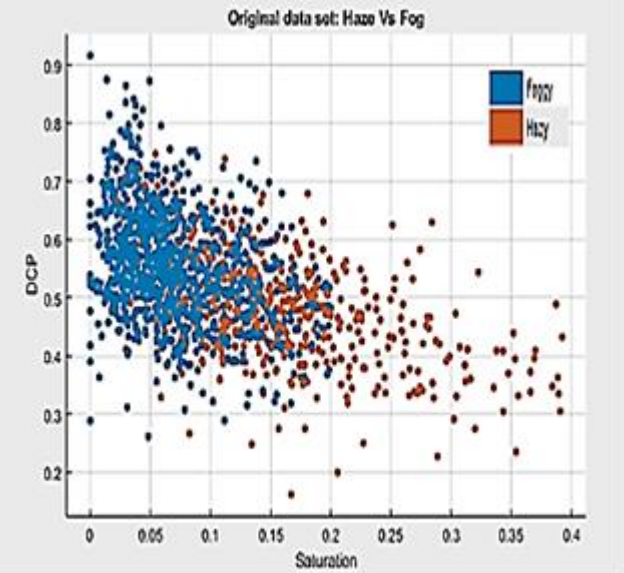

Fig 5 (a) Scatter plot (a) DCP Vs *Saturation*

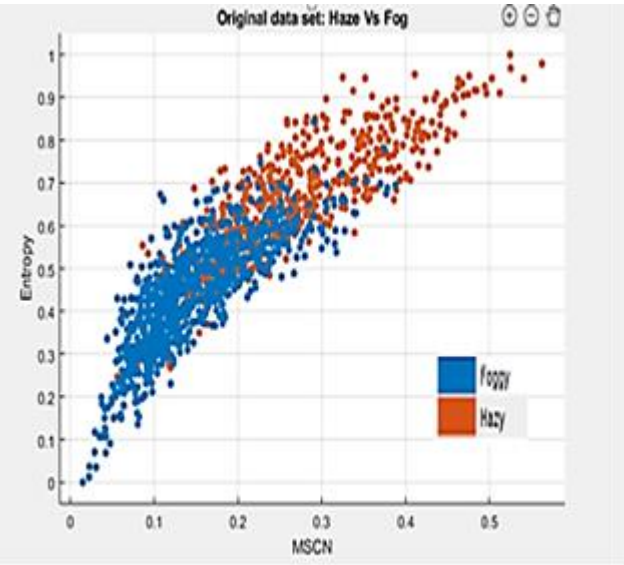

Fig. 5 (b) Entropy Vs MSCN

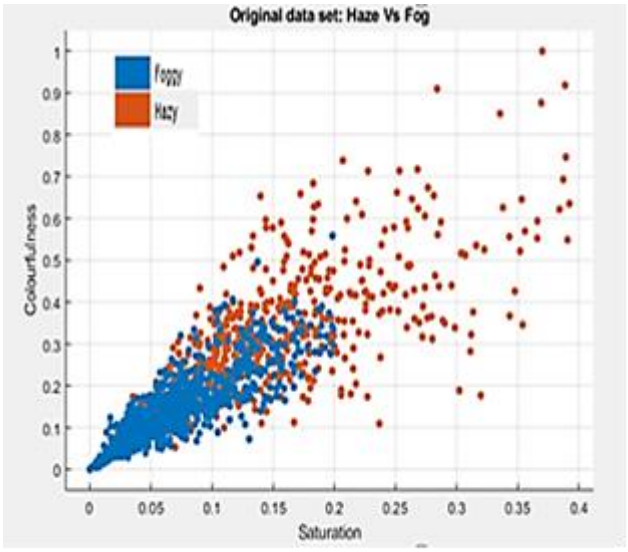

Fig 5 (c) Colorfulness Vs Saturation

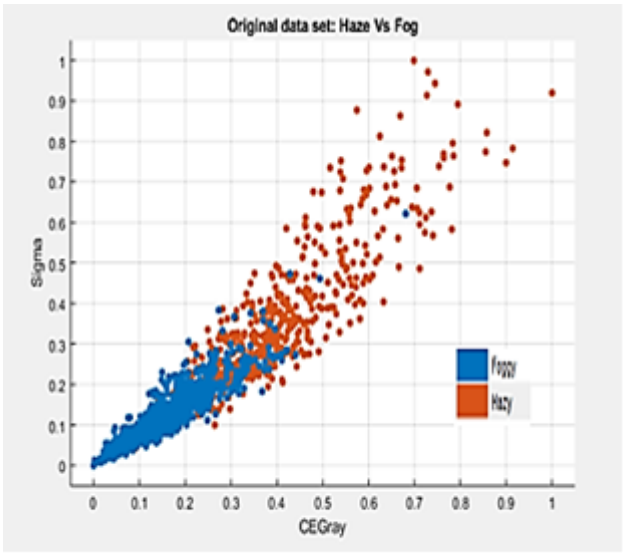

Fig 5 (d) Sharpness (Sigma) Vs Contrast Energy (gray)

3.3. Introduction to classification models

Bagging and boosting machines were the two most popular types of supervised classifiers. The basic model or predictor for the bagging and boosting machine is the decision tree. Bagging and boosting were ensemble models which had multiple decision trees.

The bagging technique was also known as bootstrap aggregation. A subset of the dataset which was drawn by random sampling with replacement method was fed to each independent predictor which was developed in parallel. The final prediction in the bagging technique was obtained by merging the average prediction of all the models or by majority voting. Random forest is an example of the bagging technique.

In the boosting technique, the predictors were developed sequentially, so that the successive predictor learns from its previous predictor so that every predictor predicted better than the previous predictor till the predictor predicts closer to the target. Adaptive Boosting (AdaBoost) and Gradient Boosting are examples of boosting techniques.

XGBoost is an acronym for an extreme gradient boosting machine. XGBoost can be used for regression or classification problems. XGBoost is a type of gradient boosting machine which functions sequentially so that the predictors are trained with the objective to reduce the loss function [27]. XGBoost is a type of gradient boosting machine intended for speed and performance. When compared with the existing classifier, the speed of XGBoost is ten times faster on a single platform. All the cores of the processor are utilized while running and can process the core in parallel. XGBoost can be implemented in multiple programming languages like Python, Java, R, and C^{++}. Regularization is an important feature in XGBoost which avoids overfitting. It is a flexible classifier where a user can set the parameters of the objective function. The classifier can deal with missing values. The objective function is defined in (5) as specified by Chen et al. [27].

$$Obj(\theta) = L(\theta) + R(\theta) \quad (5)$$

where $L(\theta)$ is the training loss which is measured to indicate how well the model fits the data and $R(\theta)$ is the regularization factor which is measured to indicate the complexity of the model.

To summarize, the XGBoost classifier is fast as it runs parallel using all the core of the machine and it also supports multiple programming languages. One of the important features of XGBoost is regularization which does not allow data overfitting.

3.4. Training and testing the classification model

It is to be noted that imbalanced classification involves developing predictive models on classification datasets that have a severe class imbalance. The new imbalanced database formed as shown in Table 1 has more sunny images. Hazy images are comparatively less and they form the minority class with sunny images as the majority class. Working with datasets of imbalanced type is very challenging and is ignored by many classifiers of machine learning. Hence the performance is poorer for the minority class though its consideration is very vital.

A way to solve this issue of imbalanced datasets is to do oversampling of the minority class. Of course, such values do not provide fresh or extra information about that model but, synthesizing new values is possible from the values already available. Such data augmenting for the minority class is the kind suggested by Chawla et al. [28] who coined the name "***Synthetic Minority Oversampling Technique" (SMOTE).*** To fix the imbalance issue in the new dataset, the minority set was oversampled using the SMOTE technique. Each class now has 1208 samples after performing SMOTE on 80% of the training dataset.

The evaluation of a classification model on the training dataset will lead to a biased score. Evaluation is performed

on the held-out sample to obtain an unbiased estimate of model. This is known as a train-test split approach for model evaluation. The training set is a set of images used to train the classification model. To improve the accuracy of the trained model the parameters are tuned during the training phase and tested using the set of images known as a validation set. Finally, the performance of a classifier is tested using another set of images unseen by the model which is known as the testing set.

Initially, the statistical features extracted from the images were used to train the model using supervised classifiers. In the proposed method 80% of the images were taken for training and 20% for testing. Out of 80%, 68% was initially used to train the model, and the rest 12% is used for validating the model. The model was trained with the dataset using different classifiers. Table 2 shows the accuracy of each classifier after training with 68% dataset and validating with 12% of the dataset to select the best classifiers.

From Table 2, we can infer from the validation accuracy, that out of six models XGBoost, Light Gradient Boosting Machine (Light GBM), Random forest and SVM classifiers perform better, on the given dataset. Thus, these four classifiers are shortlisted, and their parameters are tuned to improve the performance.

Table 2. Training and Validation Accuracy

S. No	Classifier	Training Accuracy (%)	Validation Accuracy (%)
1	Naive Bayes	79.4897	77.9036
2	Decision Tree	100	84.9858
3	Random Forest	100	90.6516
4	XGBoost	100	91.5014
5	Light GBM	100	90.9348
6	Support Vector Machine	90.7453	89.5184
7	AdaBoost	83.3916	83.0028

Stratified K-fold Cross-validation were performed on the selected top classifiers to improve accuracy with 80% dataset. Cross-validation is a statistical method used to compute the ability of a machine learning model with small dataset. Cross-validation was performed to avoid a classification model overfitting. Cross-validation is performed to select a model for the given predictive problem because it is easy to understand and implement with low bias. In the proposed method cross-validation was performed with k=5.

The procedure for performing stratified K-fold cross-validation is as follows, First, 80% of the dataset is randomly shuffled and the dataset is divided into k groups. Out of the k group, one group is set aside for testing and the remaining (k-1) group is trained. The process is repeated consecutively with different sets of (k-1) groups to train the model with the group which is set aside for testing. Each time the accuracy is measured and finally, the average accuracy is taken for consideration.

XGBoost parameters are tuned to improve the accuracy of the classifier [27]. The parameters are tuned as shown in Table 3. The learning rate is tuned which determines the step size. The depth of the decision tree is tuned to the maximum as shown in Table 3. Similarly, the n-estimator will decide the number of trees used in the proposed model. The seed is the learning parameter and n-split is used to split the dataset into k parts.

Table 3. Hyper parameters Tuned for XGBoost Classifier

S.No	XGBoost Classifier Parameters	Parameter value
1	Learning rate (α)	0.25
2	The max-depth of the decision tree	7
3	The n-estimator used in the model	75
4	The random-state parameter or seed	1234
5	The n-split	5

Similarly, Table 4 shows the parameters tuned for the Light gradient boosting machine. By tuning these parameters for both the classifiers it was found that the accuracy improved further.

Table 4. Hyper parameters Tuned for Light GBM Classifier

S.No	Light GBM Classifier Parameters	Parameter value
1	Bagging fraction	0.5
2	Learning rate	0.25
3	Maximum Bin	50
4	Maximum depth	7
5	Minimum child samples	10
6	Minimum child weight	0.1
7	Number of leaves	31

After implementing stratified K-fold Cross-Validation with K=5, XGBoost accuracy was improved to 93.7363% and the accuracy for Light GBM was 93.9292%. XGBoost and Light GBM after tuning the parameters were found to be performing equally well. Other classifiers showed less accuracy and was not considered further for testing.

4. Results and discussion

The classification algorithm was implemented using PYTHON version 3.7. The parameters were set as given in Table 3 and Table 4 and the model was tested finally with 20 % unseen data from the dataset. After testing with 20% of data it was found that XGBoost classifier outperformed. The confusion matrix represents the quality of the output of

a supervised classifier. The diagonal value represent the actual and predicted values are correct, whereas the off-diagonal values represent the actual and predicted values are incorrect. Normally an accurate classifier should have higher values in diagonal and lower values in off-diagonal to represent misclassified results. The proposed method was tested on 589 images and the confusion matrix was obtained as shown in Fig. 6.

From the confusion matrix obtained using the XGBoost classifier, it can be seen that the diagonal values show a higher value representing the accurately classified images and the off-diagonal values representing less misclassified images. The diagonal values indicate True Positive (TP) and True Negative (TN) and the off-diagonal values represent False Positive (FP) and False Negative (FN). Accuracy, precision, recall as well as F1-score can be determined using these measures.

Accuracy is an important performance metric of a classifier which is defined as the ratio of rightly predicted observations to the entire observations as in (6),

$$Accuracy = \frac{TP+TN}{TP+FP+FN+TN} \quad (6)$$

Precision is the ratio of correctly predicted positive observations to the totally predicted positive observations as depicted in (7)

$$Precision = \frac{TP}{TP+FP} \quad (7)$$

Recall or Sensitivity is the ratio of rightly predicted positive observations to the entire observations in actual positive class as depicted in (8)

$$Recall = \frac{TP}{TP+FN} \quad (8)$$

F1-Score is the weighted average of Precision and Recall as specified in (9)

$$F1\ Score = \frac{2\times(R\times P)}{(R+P)} \quad (9)$$

Equation (9) shows the F1-Score which is a function of precision and recall [29]. When precision was tuned to increase in a classifier, the recall decreased. Choosing a classifier based on their performance with these metrics will be difficult because if one classifier shows a better precision the other classifier will show a better recall, so F1-Score is an important metric to choose the best classifier. Both XGBoost and Light GBM were tested with a 20% unseen test data set, since the k-fold cross-validation accuracy of the XGBoost and Light GBM were closer after tuning the hyper parameters. The classification report of Light GBM is shown in Table 5. As shown in Table 5 the overall accuracy of the Light GBM using (6) is 89.643%.

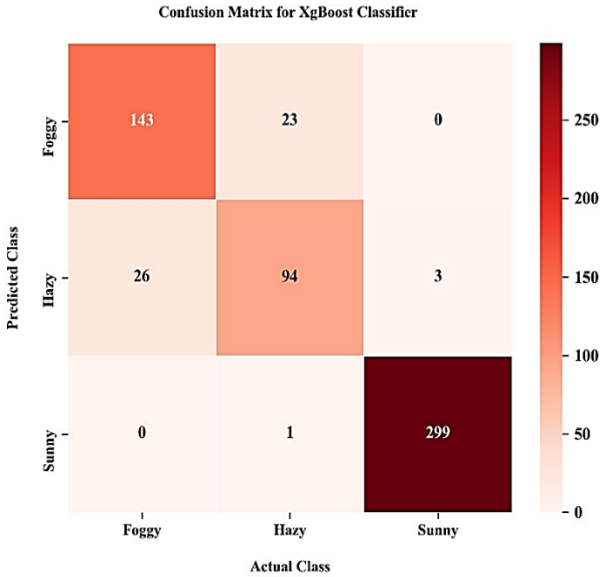

Fig. 6. Confusion Matrix obtained using XGBoost

Table 5. Classification Report of Light GBM classifier for each class

Weather category	Precision %	Recall %	F1-Score %	Accuracy %
Foggy	85.185	81.657	83.383	81.656
Hazy	72.441	77.966	75.102	77.966
Sunny	99.333	98.675	99.003	98.675
Overall Testing accuracy of Light GBM classifier				89.643

Similarly, Table 6 shows the classification report for each class using the XGBoost classifier. From Table 6 it can be seen that the overall accuracy of the XGBoost classifier for classifying the static weather images using (6) is 91%. Precision, recall, F1-score measures are calculated using (7), (8) and (9) respectively. Table 6 specifies precision, recall and F1-score per class obtained from XGBoost classifier.

Table 6. Classification Report of XGBoost classifier for each class

Weather category	Precision %	Recall %	F1-Score %	Accuracy %
Foggy	86.144	84.615	85.373	84.615
Hazy	76.422	79.661	78.008	79.661
Sunny	99.667	99.006	99.335	99.006
Overall Testing accuracy of XGBoost classifier				91.0017

Receiver Operating Characteristic (ROC) curve is a plot between the True Positive Rate (TPR) and False Positive Rate (FPR). In other words, it is a plot between sensitivity and (1-specificity). An excellent model has Area under the Curve (AUC) closer to one. The implication is there exists a separability measure which is better. An AUC nearer to zero shows a poorer model. It possesses a separability measure that is very bad and can also be said to be the worst. In particular, while AUC is 0.5, it amounts to stating that a

specific model possesses no class separation capacity at all. Fig.7, Fig. 8, and Fig. 9 depict the ROC curves obtained using an XGBoost classifier. The accuracy of the prediction is determined from the Area Under the Curve (AUC) with the higher value indicating more accuracy of the prediction. The AUC for foggy is 0.88, for hazy 0.87, and the AUC for sunny is 0.99.

Feature importance or feature score denote the methods that assign a score to statistical features based on how useful they are at classifying the weather images. Table 7 shows the feature score for various statistical features and the same is plotted in Fig. 10. Fig.10 clearly shows that the features like saturation, contrast energy and sharpness are useful in classifying the static weather images when compared to the other statistical features.

Table 7. Feature score for each statistical feature

S.No	Statistical features	Feature score
1.	MSCN	0.03878
2.	Entropy	0.02820
3.	Dark channel prior(DCP)	0.03913
4.	Colourfulness	0.04382
5.	Contrast Energy (gray)	0.23451
6.	Saturation	0.39524
7	Contrast energy (blue-yellow)	0.11672
8	Contrast energy (red-green)	0.02964
9	Sharpness	0.07396

Fig. 7. ROC curve for foggy images obtained using XGBoost

Fig. 8. ROC curve for hazy images obtained using XGBoost

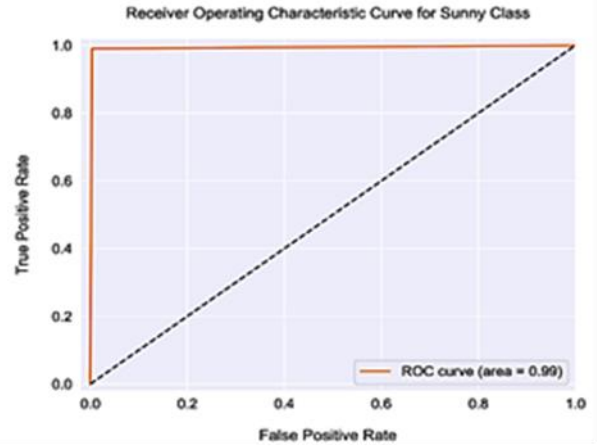

Fig. 9. ROC curve for sunny images obtained using XGBoost

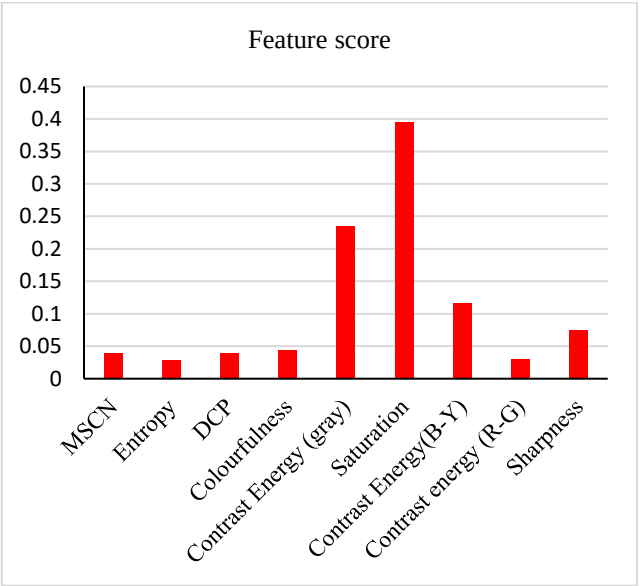

Fig. 10. Plot showing the feature score for each statistical feature

Fig. 11. Classification results (a) to (d) Sunny images, (e) to (h) Hazy images, and (i) to (l) Foggy images

(a) Sunny image predicted as hazy

(b) Hazy image predicted as foggy

(c) Foggy image predicted as Hazy

Fig. 12. Misclassified images.

Fig. 11 shows sample images correctly classified by the classifier. Contrast and color were observed more for sunny images whereas for hazy and foggy images the contrast decreased gradually.

A few images were misclassified as shown in Fig. 12. Based on observation, it was found that the misclassification happens when the image has a background scene with more white objects as shown in Fig.12 (a) where the actual image is a sunny image predicted as a hazy image. Similarly, if a hazy image has a background scene with more white objects then they are misclassified as foggy. Fig. 12 (b) was misclassified as foggy but the actual image is hazy where

the background scene is visible. Misclassification is due to the reflection of the cloudy sky that has caused the water in the lake to be bright, similar to fog. Foggy image is misclassified as hazy when the scene is covered with more objects closer to the camera and more visible as shown in Fig.12 (c).

5. Conclusion

The proposed static weather image classification model has pioneering opportunity to analyze fog and haze as two separate classes. Other researchers have been treated them as one class so far. The proposed method was implemented by collecting images from the existing databases and forming a new database by relabelling the images as haze and fog based on psycho-visual analysis. From the feature score, we can conclude that statistical features like saturation, contrast energy, sharpness dominate when compared to the other features thereby enhancing the classifier. The accuracy obtained from the proposed method using the XGBoost classifier was 91%.

The high speed and performance of the XGBoost classifier is a perfect choice for implementing this classifier in any autonomous navigation system.

In future, the classification can be extrapolated for dynamic weather images like rain and snow. The accuracy can be further enhanced by classifying foggy and cloudy images which will throw a challenge for the researchers who are pursuing this field. The work can also be extended by classifying heterogeneous hazy and foggy images. From the misclassified image it was also observed that the proposed method was not able to distinguish a white object in an image from haze or fog. On the other hand, a foggy image is misclassified as hazy, if a greater number of objects closer to the camera are visible in the foggy image. To tide over such obstacles the work can be extended by considering features to detect white objects and the objects with respect to depth of the image, in the future.

References

[1]. Nayar, S. K., & Narasimhan, S. G. "Vision in bad weather". In *Proceedings of the Seventh IEEE International Conference on Computer Vision* .Vol. 2, pp. 820-827, IEEE, September 1999.

[2]. Ju, M., Ding, C., Ren, W., Yang, Y., Zhang, D., & Guo, Y. JIde: "Image dehazing and exposure using an enhanced atmospheric scattering model", *IEEE Transactions on Image Processing*, *30*, 2180-2192, 2021.

[3]. Kadhim, R. R., and M. Y. Kamil. "Evaluation of Machine Learning Models for Breast Cancer Diagnosis Via Histogram of Oriented Gradients Method and Histopathology Images". International Journal on Recent and Innovation Trends in Computing and Communication, vol. 10, no. 4, Apr. 2022, pp. 36-42, doi:10.17762/ijritcc.v10i4.5532.

[4]. Zhang, Y., Zhang, J., Huang, B., & Fang, Z. ,"Single-image deraining via a recurrent memory unit network" *Knowledge-Based Systems*, *218*, 106832, 2021.

[5]. Hautiere, N., Tarel, J. P., Lavenant, J., & Aubert, D., "Automatic fog detection and estimation of visibility distance through use of an onboard camera". *Machine vision and applications*, *17*(1), 2006

[6]. L. N. Balai, G. K. J. A. K. S. (2022). Investigations on PAPR and SER Performance Analysis of OFDMA and SCFDMA under Different Channels. International Journal on Recent Technologies in Mechanical and Electrical Engineering, 9(5), 28–35. https://doi.org/10.17762/ijrmee.v9i5.371

[7]. Lagorio, A., Grosso, E., & Tistarelli, M, "Automatic detection of adverse weather conditions in traffic scenes" In *2008 IEEE Fifth International Conference on Advanced Video and Signal Based Surveillance* (pp. 273-279) IEEE, September 2008.

[8]. Negru, M., & Nedevschi, S. "Image based fog detection and visibility estimation for driving assistance systems", In *2013 IEEE 9th International Conference on Intelligent Computer Communication and Processing (ICCP)* (pp. 163-168). IEEE, September 2013.

[9]. Shen, L., & Tan, P, "Photometric stereo and weather estimation using internet images". In *2009 IEEE Conference on Computer Vision and Pattern Recognition* (pp. 1850-1857). IEEE, June, 2009.

[10]. Cord, A., & Aubert, D, "Towards rain detection through use of in-vehicle multipurpose cameras". In *2011 IEEE Intelligent Vehicles Symposium (IV)* (pp. 833-838). IEEE, June, 2011.

[11]. Roser, M., & Moosmann, F, "Classification of weather situations on single color images". In *2008 IEEE Intelligent Vehicles Symposium* (pp. 798-803). IEEE, June 2008.

[12]. S, R. D., L. . Shyamala, and S. . Saraswathi. "Adaptive Learning Based Whale Optimization and Convolutional Neural Network Algorithm for Distributed Denial of Service Attack Detection in Software Defined Network Environment". International Journal on Recent and Innovation Trends in Computing and Communication, vol. 10, no. 6, June 2022, pp. 80-93, doi:10.17762/ijritcc.v10i6.5557.

[13]. Yan, X., Luo, Y., & Zheng, X.,"Weather recognition based on images captured by vision system in vehicle". In *International Symposium on Neural Networks* (pp. 390-398). Springer, Berlin, Heidelberg, May, 2009.

[14]. Elhoseiny, M., Huang, S., & Elgammal, A,"Weather classification with deep convolutional neural networks". In *2015 IEEE International Conference on Image Processing (ICIP)* (pp. 3349-3353). IEEE, September, 2015.

[15]. Zhang, Z., Ma, H., Fu, H., & Zhang, C "Scene-free multi-class weather classification on single images". *Neurocomputing*, *207*, 365-373, 2016.

[16]. Chu, W. T., Zheng, X. Y., & Ding, D. S, "Camera as weather sensor: Estimating weather information from single images". *Journal of Visual Communication and Image Representation*, *46*, 233-249, 2017.

[17]. Wang, S., Tian, Y., Pu, T., Wang, P., & Perner, P, 'A hazy image database with analysis of the frequency magnitude", *International Journal of Pattern*

Recognition and Artificial Intelligence, *32*(05), 1854012, 2018.

[18]. Choi, L. K., You, J., & Bovik, A. C "Referenceless prediction of perceptual fog density and perceptual image defogging. *IEEE Transactions on Image Processing*, *24*(11), 3888-3901, 2015.

[19]. Sheikh, H. R., Sabir, M. F., & Bovik, A. C, "A statistical evaluation of recent full reference image quality assessment algorithms", *IEEE Transactions on image processing*, *15*(11), 3440-3451, 2006.

[20]. Kiran, M. S., & Yunusova, P. (2022). Tree-Seed Programming for Modelling of Turkey Electricity Energy Demand. International Journal of Intelligent Systems and Applications in Engineering, 10(1), 142–152. https://doi.org/10.18201/ijisae.2022.278

[21]. Martin, D., Fowlkes, C., Tal, D., & Malik, J, "A database of human segmented natural images and its application to evaluating segmentation algorithms and measuring ecological statistics". In *Proceedings Eighth IEEE International Conference on Computer Vision. ICCV 2001* (Vol. 2, pp. 416-423). IEEE, July, 2001.

[22]. Ghazaly, N. M. . (2022). Data Catalogue Approaches, Implementation and Adoption: A Study of Purpose of Data Catalogue. International Journal on Future Revolution in Computer Science &Amp; Communication Engineering, 8(1), 01–04. https://doi.org/10.17762/ijfrcsce.v8i1.2063

[23]. Le Callet, P., & Autrusseau, F, "Subjective quality assessment IRCCyN/IVC database", .2005.

[24]. Larson, Eric Cooper, and Damon Michael Chandler, "Most apparent distortion: full-reference image quality assessment and the role of strategy", Journal of electronic imaging 19.1, 2010: 011006, 2010.

[25]. Tan, R. T "Visibility in bad weather from a single image". In *2008 IEEE Conference on Computer Vision and Pattern Recognition* (pp. 1-8). IEEE. , June, 2008.

[26]. Fattal, R "Single image dehazing". *ACM transactions on graphics (TOG)*, *27*(3), 1-9, 2008.

[27]. He, K., Sun, J., & Tang, X, "Single image haze removal using dark channel prior". *IEEE transactions on pattern analysis and machine intelligence*, *33*(12), 2341-2353, 2010.

[28]. Tarel, J.P., & Hautiere, N, "Fast visibility restoration from a single color or gray level image". In *2009 IEEE 12th international conference on computer vision* (pp. 2201-2208). IEEE, September 2009.

[29]. Kratz, L., & Nishino, K, "Factorizing scene albedo and depth from a single foggy image". In *2009 IEEE 12th International Conference on Computer Vision* (pp. 1701-1708) IEEE, September, 2009.

[30]. Nishino, K., Kratz, L., & Lombardi, S, "Bayesian defogging". *International journal of computer vision*, *98*(3), 263-278, 2012.

[31]. Ancuti, C. O., & Ancuti, C, "Single image dehazing by multi-scale fusion", *IEEE Transactions on Image Processing*, *22*(8), 3271-3282, 2013.

[32]. Chen, T., & Guestrin, C. "Xgboost: A scalable tree boosting system". In *Proceedings of the 22nd acm sigkdd international conference on knowledge discovery and data mining* (pp. 785-794), August, 2016.

[33]. Chawla, N. V., Bowyer, K. W., Hall, L. O., & Kegelmeyer, W. P. "SMOTE: synthetic minority over-sampling technique". *Journal of artificial intelligence research*, *16*, 321-357, 2002.

[34]. Fawcett, T, "An introduction to ROC analysis". Pattern recognition letters, 27(8), 861-874, 2006.